Multistep Prediction of Physiological Tremor Based on Machine Learning for Robotics Assisted Microsurgery

Sivanagaraja Tatinati, *Student Member, IEEE*, Kalyana C. Veluvolu, *Senior Member, IEEE*, and Wei Tech Ang, *Member, IEEE*

***Abstract*—For effective tremor compensation in robotics assisted hand-held device, accurate filtering of tremulous motion is necessary. The time-varying unknown phase delay that arises due to both software (filtering) and hardware (sensors) in these robotics instruments adversely affects the device performance. In this paper, moving window-based least squares support vector machines approach is formulated for multistep prediction of tremor to overcome the time-varying delay. This approach relies on the kernel-learning technique and does not require the knowledge of prediction horizon compared to the existing methods that require the delay to be known as *a priori*. The proposed method is evaluated through simulations and experiments with the tremor data recorded from surgeons and novice subjects. Comparison with the state-of-the-art techniques highlights the suitability and better performance of the proposed method.**

***Index Terms*—Least squares support vector machines (LS-SVM), multistep prediction, physiological motions, tremor.**

I. Introduction

PHYSIOLOGICAL tremor defined as an involuntary, roughly sinusoidal component inherent in normal hand motion. It has multiple dominant frequencies usually distributed between 6 to 14 Hz with an amplitude of 50 to 100 μm in each principal axis [1]–[4]. The dominant frequencies of physiological tremor are usually limited to 4 Hz bandwidth (for e.g., 8–12 Hz for a typical healthy subject) [4]–[8]. The analysis conducted on physiological tremor time series in [4]–[6] and [9]–[12] suggested that tremor is nonstationary in nature and exhibits significant variations in amplitude, frequency, and bandwidth over the time. Physiological tremor is the main cause for human imprecision during microsurgery [1], [13]. Microsurgery requires precise manual positioning of hand, for e.g., vitreoretinal microsurgery requires a positioning accuracy of 10 μm [3]. Presence of physiological tremor adversely affects the efficacy of surgeon and restricts the number of qualified microsurgeons [1], [13]. Thereby, to improve the performance of microsurgeon, several techniques based on robotics have been proposed [2], [14]–[18]. Of these techniques, hand-held robotic instruments can retain the skills possessed by the surgeons and augment the tip positioning accuracy in real-time [18], [19]. Further, recent studies showed that micro surgeons tremor characteristics differ from normal subjects and the cancellation of former's tremor with robotics is more challenging [4], [15].

In typical hand-held instruments [19], the tremor compensation comprises of three stages: 1) sensing (with accelerometers); 2) filtering and modeling (to separate voluntary and tremulous motions); and 3) compensation (canceling the tremulous motion with opposite actuation). For effective tremor compensation, all the three stages have to be accomplished in one cycle without any phase lag. The meticulous nature of the microsurgical procedures restrict the voluntary movements to low frequency components i.e., less than 2 Hz [20]. Thus, in hand-held instruments, to separate the tremulous motion from voluntary motion, noise and other disturbances, a bandpass filter with pass band (2–20 Hz) was employed [19]. Due to the presence of the linear filter in the process, time-varying phase delay of 12–16 ms is introduced into the process. Furthermore, a hardware low-pass filter in the accelerometers adds an additional 4 ms to this delay. More details are provided in Section II-C.

Recently, several signal processing algorithms have been developed to model and predict physiological tremor with the aid of robotic devices [4], [5], [14], [15], [21]. Comparative performance of all tremor prediction algorithms was provided in [5]. Band-limited multiple Fourier linear combiner (BMFLC) with Kalman filter (KF) (BMFLC-KF), and autoregressive model (AR) with KF (AR-KF) outperform other algorithms [5]. Although the methods provide a good prediction accuracy, the performance is adversely affected in the presence of phase delay. Tatinati *et al.* [5] and Veluvolu *et al.* [8] have documented the effect of phase delay on the tremor compensation in surgical robotics applications. As a solution to overcome the phase delay, multistep prediction of tremor with modifications

Manuscript received June 19, 2014; revised September 4, 2014 and November 17, 2014; accepted December 4, 2014. Date of publication December 25, 2014; date of current version January 13, 2015. This work was supported in part by the Basic Science Research Program through the National Research Foundation of Korea (NRF) and in part by the Ministry of Education, Science, and Technology under Grant NRF-2014R1A1A2A10056145. This paper was recommended by Associate Editor Z.-G. Hou. *(Corresponding author: Kalyana C. Veluvolu.)*

S. Tatinati and K. C. Veluvolu are with the School of Electronics Engineering, College of IT Engineering, Kyungpook National University, Daegu 702-701, Korea (e-mail: veluvolu@ee.knu.ac.kr).

W. T. Ang is with the School of Mechanical and Aerospace Engineering, Nanyang Technological University, Singapore.

Color versions of one or more of the figures in this paper are available online at http://ieeexplore.ieee.org.

Digital Object Identifier 10.1109/TCYB.2014.2381495

2168-2267 © 2014 IEEE. Personal use is permitted, but republication/redistribution requires IEEE permission.
See http://www.ieee.org/publications_standards/publications/rights/index.html for more information.

Authorized licensed use limited to: Huazhong University of Science and Technology. Downloaded on September 23,2024 at 07:33:24 UTC from IEEE Xplore. Restrictions apply.

to BMFLC-KF (MS-BMFLC-KF) and AR-KF (MS-AR-KF) have been proposed in [8]. These methods require the actual knowledge of the prediction horizon for accurate estimation. Furthermore, both the methods assume the process to be nonstationary in the given prediction horizon. In [8], a constant prediction horizon of 20 ms is employed to perform multistep prediction with both the methods. Since the tremor characteristics are time-varying (surgeon dependent) within the frequency band of 6–14 Hz, phase delay of band pass filtered tremor signal varies in the range of 12–20 ms and cannot be estimated in real-time. The time-varying phase delay in filtering process significantly effects the prediction performance of both MS-BMFLC-KF and MS-AR-KF. Hence a method that can model and predict tremor without any prior knowledge of prediction horizon is required to improve the prediction performance.

To address these issues, in this paper, machine learning technique is employed to perform multistep prediction of tremor without any prior knowledge of the prediction horizon. Machine learning techniques embody nontrivial relationships with the training data in order to interpret the testing data [22]. These techniques have been successfully applied in many domains such as pattern recognition and classification [23], [24], object detection and localization [25], [26], and prediction of physiological signals like respiration [27]. In this paper, to perform tremor prediction least squares support vector machines (LS-SVM) is employed. The method has been popular for classification, function estimation/system identification and time series prediction [28]–[31].

In time series prediction applications, LS-SVM formulates a nonlinear mapping between the input data and the corresponding output data in offline [32], [33]. The obtained nonlinear mapping is then employed for online prediction [32], [33]. The performance of LS-SVM relies on the correlation between the training data and the data employed for prediction. For nonstationary signals such as tremor, this technique does not guarantee good performance due to weak correlation. On the other hand, updating the nonlinear mapping with the new data at every iteration results in increasing the computational complexity. A moving window-based LS-SVM (MWLS-SVM) is developed for multistep prediction of tremor in this paper. By updating the nonlinear mapping at every iteration, the method can adapt to the time-varying characteristics of tremor. Further, this procedure does not require the knowledge of prediction horizon like earlier methods. Analysis was conducted on the tremor data collected from five surgeons and five novice subjects to validate the proposed method. The performance of the method is validated thru simulations and experiments. Results show that, the proposed method provides better prediction accuracy compared to the state-of-the-art techniques.

The rest of this paper is organized as follows. In Section II, the brief description of LS-SVM and the proposed online training approach are discussed. Section III provides tremor data collection procedure, obtained results and implications. Later, discussions are provided in Section IV, while Section V concludes this paper.

II. Materials and Methods

In this section, we first discuss the physiological tremor data collection procedure from surgeons and novice subjects that is used for analysis in this paper. Later, the methods formulated for multistep prediction are discussed.

A. Physiological Tremor Data Collection

1) Experimental Setup: Tremor recordings were performed through the micro motion sensing system (M2S2) and a sensorized stylus [6]. M2S2 provides a measurement in a $10 \times 10 \times 10$ mm^3 workspace, with a resolution of 0.7 μm and minimum accuracy of 98% [34]. The sensorized stylus is designed with similar mass characteristics to a typical surgical instrument and a reflector ball at its tip. M2S2 calculates the 3-D displacement of the ball inside the workspace using the centroid position of the infrared rays that are reflected from the ball and strike the photo sensitive diodes. For more details about the design of M2S2 and stylus and the data acquisition with M2S2, please refer to [6] and [34].

2) Experimental Protocol: Two types of tasks are performed by the subjects [6].

1) *Pointing Task:* In this task, two dots were displayed on the monitor screen. One dot is white in color and fixed while the another dot is orange in color, the latter will move according to the user‘s tool tip movement. The subject was then instructed to keep the orange dot overlapping the white dot for 30s.
2) *Tracing Task:* At the beginning of this task, a circle with 4 mm diameter was displayed on the monitor screen. The subject was then instructed to trace the circumference of the circle in clockwise direction as accurately as possible for 30s with the speed that is realistic for surgical micro manipulation tasks.

Each task was performed with three magnifications: 1) 1 x; 2) 10 x; and 3) 20 x, and with three different levels of grip force: 1) 1–2 *N*; 2) 2.5–3.5 *N*; and 3) 4–5 *N*. Subjects performed two trials for each different setting with approximately 1 min break in between. Sampling frequency of 500 Hz was employed. For more information about magnification and force conditions, see [6].

The time-frequency characteristics of surgeons and novice subjects were analyzed in [15]. It was shown that the tremor profile and time-frequency characteristics are different for surgeons and novice subjects. Surgeons tremor profile is more complex with a distributed spectrum and of low amplitude as compared to the novice subjects [15]. In [6], it was reported that grip force level has no effect on physiological tremor amplitude whereas magnification with 10 x showed a marginal decrease in amplitude of physiological tremor irrespective of the task performed. For the performance analysis in this paper, we chose three trails per task performed (pointing task, tracing task). Further, for each task, trials performed with different magnification level (1 x, 10 x, and 20 x) and same grip force (1–2 *N*) were chosen. Tremor data of five surgeons and five novice subjects with six trials per subject were considered for analysis in this paper. For more details about trials selection, see [5], [6], [15].

Authorized licensed use limited to: Huazhong University of Science and Technology. Downloaded on September 23,2024 at 07:33:24 UTC from IEEE Xplore. Restrictions apply.

B. Methods

In this subsection, the basic formulation of LS-SVM followed by the proposed framework for online training with LS-SVM are described.

1) Standard LS-SVM: SVM map the input data into a higher-dimensional feature space via a nonlinear mapping $\varphi(\cdot)$ and then perform the linear regression [32], [33]. Accordingly, regression approximation addresses the problem of estimating a function based on given training data $\{\boldsymbol{x}_i, y_i\}_{i=1}^{N}$ with $\boldsymbol{x}_i$ as n input vector of dimension n and y_i as the corresponding output. The regression model for LS-SVM can be given in the form

$$y = \mathbf{w}^T \varphi(\boldsymbol{x}) + b \tag{1}$$

where $\mathbf{w}$ is the weight vector and b is the bias.

LS-SVM is the least squares version of SVM. In LS-SVM, Vapnik's insensitive loss function has been replaced by a mean square error cost function [33]. Due to this reformulation, the optimal solution with LS-SVM is obtained directly by solving a set of linear equations rather than a convex quadratic program. Furthermore, this reformulation reduces the computational complexity significantly.

The optimization problem for the function estimation with LS-SVM is defined as follows:

$$\min_{\mathbf{w},b,e} J(\mathbf{w}, e) = \frac{1}{2}\mathbf{w}^T\mathbf{w} + C\sum_{i=1}^{N} e_i^2 \tag{2}$$

subject to the constraints $y_i = \mathbf{w}^T\varphi(\boldsymbol{x}_i) + b + e_i$; $i = 1, 2, \ldots, N$; where C is a regularization constant and e_i is the estimation error.

The Lagrangian function for the optimization problem can be given as

$$L(\mathbf{w}, b, e; \alpha) = J(\mathbf{w}, e) - \sum_{i=1}^{N} \alpha_i \left[\mathbf{w}^T\varphi(\boldsymbol{x}_i) + b + e_i - y_i\right] \tag{3}$$

where $\alpha = [\alpha_1, \alpha_2, \ldots, \alpha_N]$ represents the Lagrangian multipliers.

The Karush–Kuhun–Tucker (KKT) [33] conditions for the optimization problem are given as

$$\left.\begin{array}{lll} \frac{\partial L}{\partial \mathbf{w}} = 0 & \rightarrow & \mathbf{w} = \sum_{i=1}^{N} \alpha_i \varphi(\boldsymbol{x}) \\ \frac{\partial L}{\partial e_i} = 0 & \rightarrow & \alpha_i = Ce_i \\ \frac{\partial L}{\partial b} = 0 & \rightarrow & \sum_{i=1}^{N} \alpha_i = 0 \\ \frac{\partial L}{\partial \alpha_i} = 0 & \rightarrow & \mathbf{w}^T\varphi(\boldsymbol{x}_i) + b + e_i - y_i = 0 \end{array}\right\}. \tag{4}$$

After eliminating e_i and $\mathbf{w}$ from (3) by using the KKT conditions (4), the optimization solution becomes a set of linear equations, given as

$$\delta_N = \Psi_N^{-1}\ \mathbf{y}_N \tag{5}$$

where $\delta_N = [b, \alpha_1, \ldots, \alpha_N]^T$; $\overrightarrow{\mathbf{1}} = [1, 1, \ldots, 1]^T$; $\mathbf{y} = [y_1, y_2, \ldots, y_N]^T$; $\Psi_N = \begin{bmatrix} 0 & \overrightarrow{\mathbf{1}}^T \\ \overrightarrow{\mathbf{1}}^T & \Omega + \mathbf{C^{-1}}\boldsymbol{I} \end{bmatrix}$ and Ω follows Mercer's condition [33] i.e., $\Omega_{ij} = K(\boldsymbol{x}_i, \boldsymbol{x}_j) = \varphi(\boldsymbol{x}_i)^T\varphi(\boldsymbol{x}_j)$; $i, j = 1, 2, \ldots, N$ and $K(\cdot, \cdot)$ represents the kernel function. In this paper, RBF kernel function is employed, can be defined as $K(\boldsymbol{x}, \boldsymbol{x}_i) = \exp\{-||\boldsymbol{x} - \boldsymbol{x}_i||^2/\sigma^2\}$.

From (1) and (5), the prediction model with LS-SVM is obtained as

$$\hat{y}(k+T) = \sum_{i=1}^{N} \alpha_i K(\boldsymbol{x}_i, \boldsymbol{x}_k) + b;\ \ k = N+1, \ldots, l \tag{6}$$

where b and α are from (5) and l is the length of test signal.

Although LS-SVM has been popular for time series prediction and financial forecasting, its performance is not effective when the signal characteristics often change with time. Recently, in [27], an online training method for SVM was implemented for respiratory motion prediction. However, this method focuses on incrementing the training set with the available new sample. Further, respiratory motion is semi periodic in nature with slow-varying characteristics (frequency range < 1 Hz). Physiological tremor is a quasi periodic signal and lies in the high frequency range (6–14 Hz). Together with the nonstationary characteristics, the multistep prediction becomes much more challenging with LS-SVM compared to the other physiological motions like respiratory motions.

To address these issues, MWLS-SVM is proposed in next subsection.

2) MWLS-SVM: Compared to the existing variants of LS-SVM [28], [29], the main difference of the proposed method lies in updating the training set and the parameters α, b for every iteration, thereby reducing the computational complexity. A fixed window length is maintained by discarding the oldest sample from training set, as shown in Fig. 1. To avoid matrix inversion (Ψ_N^{-1}) and to decrease the computational complexity, incremental algorithm is employed to increment the training set and decremental algorithm to discard the oldest sample. This moving window training approach allows LS-SVM to track the nonstationary dynamics in tremor signal more effectively without increasing the computational complexity.

The incremental and decremental algorithms employed for MWLS-SVM are discussed below.

Let $(\boldsymbol{x}_{N+1},\ y_{N+1})$ be a new data pair, then the incremental algorithm updates the trained LS-SVM (of N data pairs) by adding the new data pair and then computes the inverse of the matrix Ψ_N in (5), for $N+1$ data pairs (Ψ_{N+1}), without explicitly calculating the inverse. From (5), the optimal solution with the incremented training set ($N+1$ data pairs) is

$$\delta_{N+1} = \Psi_{N+1}^{-1}\ \mathbf{y}_{N+1} \tag{7}$$

where $\delta_{N+1} = [b, \alpha_1, \ldots, \alpha_N, \alpha_{N+1}]^T$; $\Psi_{N+1} = \begin{bmatrix} \Psi_N & \mathbf{a} \\ \mathbf{a}^T & c \end{bmatrix}$; $\mathbf{y}_{N+1} = [\mathbf{y}_N\ \ \hat{y}_{k+T}]^T$; and $\mathbf{a} = [1; K(\boldsymbol{x}_1; \boldsymbol{x}_{N+1}); \cdots; K(\boldsymbol{x}_N, \boldsymbol{x}_{N+1})]$.

Incremental algorithm updates Ψ_{N+1}^{-1} from Ψ_N^{-1} without the explicit computation of the matrix inverse. The mathematical proof for calculating the augmented matrix is well documented [35] and the main result is reproduced here for convenience of readers

$$\Psi_{N+1}^{-1} = \begin{bmatrix} \Psi_N^{-1} & \mathbf{0}^T \\ \mathbf{0} & 0 \end{bmatrix} + \left[c - \mathbf{a}^T\Psi_N^{-1}\mathbf{a}\right]^{-1} \begin{bmatrix} \Psi_N^{-1}\mathbf{a} \\ -1 \end{bmatrix} \left[\mathbf{a}^T\Psi_N^{-1} - 1\right] \tag{8}$$

Authorized licensed use limited to: Huazhong University of Science and Technology. Downloaded on September 23,2024 at 07:33:24 UTC from IEEE Xplore. Restrictions apply.

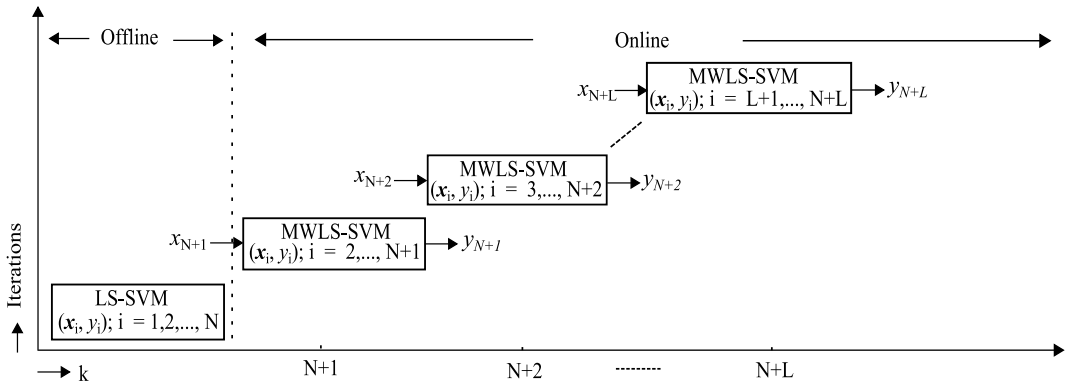

Fig. 1. Block diagram representation for tremor prediction with MWLS-SVM.

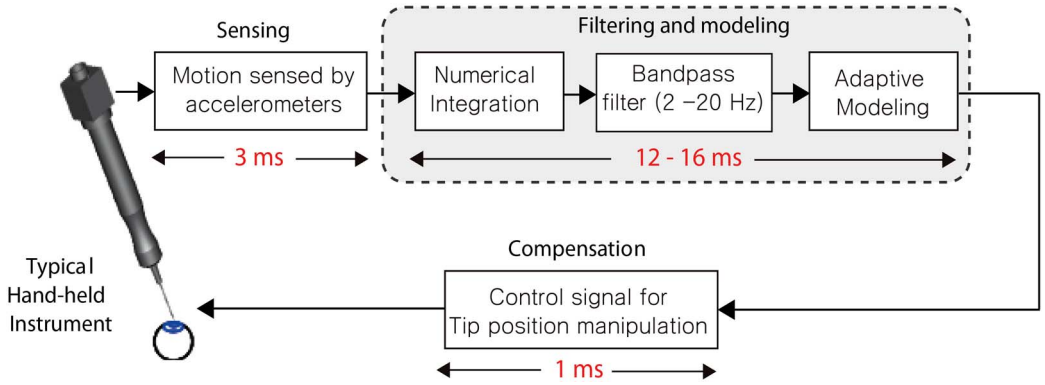

Fig. 2. Latency in the tremor compensation.

where Ψ_N^{-1} is obtained from trained LS-SVM, while c and $\mathbf{a}$ are obtained from (7).

Similar to the incremental algorithm, to avoid matrix inversion while discarding the oldest sample, Ψ_N^{-1} is updated from Ψ_{N+1}^{-1}, here Ψ_N^{-1} is the inversion of matrix Ψ_{N+1} without kth row and kth column.

Let $(\boldsymbol{x}_k, y_k)$ be the data pair that is to be removed from the $N+1$ existing data pairs. Without the explicit calculation of the matrix inversion for the N data pairs, the following update is employed [29]:

$$\Psi_{ij}^{-1} = \Psi_{ij}^{-1} - \frac{\Psi_{ik}^{-1}\Psi_{kj}^{-1}}{\Psi_{kk}^{-1}} \tag{9}$$

where $i, j = 1, \ldots, N$; $i, j \neq k$, Ψ_{ij}^{-1} stands for ith row and jth column of Ψ_{N+1}^{-1}.

From (5), the corresponding Lagrangian multipliers and bias values are computed for the updated N data pairs. With the updated Lagrangian multipliers and bias, prediction is performed with (6).

C. Tremor Prediction With MWLS-SVM

Tremor compensation mechanism employed in hand-held instrument [19] is shown in Fig. 2. In this device, accelerometers form the core part for sensing the maneuvered motion due to its small size and versatility. The sensed motion from the accelerometers is in acceleration domain, numerical double integration is required to obtain the position domain. A fifth order Butterworth bandpass filter with a pass band of 2–20 Hz is employed to separate the tremulous motion from intended motion and also to eliminate the unwanted integration drift obtained while converting acceleration to position domain. The filtered tremor signal is adaptively modeled to generate an opposing motion to compensate tremor. The compensation was performed thru piezo electric actuators in the position domain.

Although the filtering and estimation of tremor signal is effective and accurate, real-time tremor compensation with hand-held instruments is hampered by other factors such as phase delay, drift, and noise. Of these, phase delay is the major factor that affects the tremor compensation adversely in real-time [5]. The prime source for this phase delay is the employment of linear filters in the tremor filtering and compensation procedure [15], [34]. In the sensing stage, a delay of 3 ms was identified due to the presence of an on-board low-pass filter in accelerometers. Further, the band pass filter employed in the filtering and modeling stage introduces a time varying delay of 12–16 ms. An additional delay of 1 ms is identified while performing compensation with the piezo electric actuators. Thus, a total delay in the range of 16–20 ms is unavoidable from sensing to compensation in hand-held instruments. Although, the delays from sensing and compensation stages are constant, the filtering and modeling stage introduces frequency dependent delay (time varying phase delay).

The proposed approach updates the formulated offline nonlinear mapping with moving window approach at every iteration. To form the nonlinear mapping for delay, MWLS-SVM is trained offline with N samples of bandpass filtered tremor data and zero-phase band pass filtered tremor

Authorized licensed use limited to: Huazhong University of Science and Technology. Downloaded on September 23,2024 at 07:33:24 UTC from IEEE Xplore. Restrictions apply.

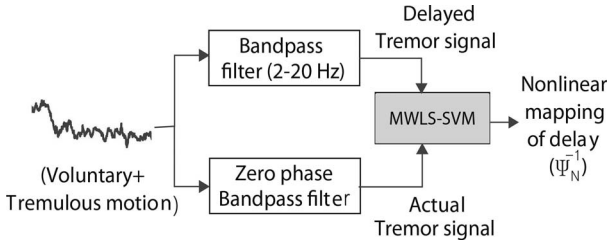

Fig. 3. Offline training for MWLS-SVM.

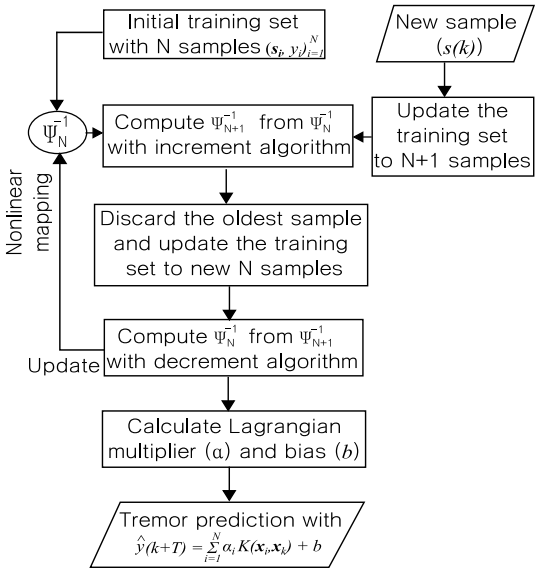

Fig. 4. Flowchart representation of MWLS-SVM.

data as shown in Fig. 3. The nonlinear mapping (Ψ_N^{-1}) and the corresponding parameters (α and b) are calculated offline with (5) as shown in Fig. 3. Ahead prediction of tremor can be performed with the obtained nonlinear mapping as shown in (6).

In real-time, with the arrival of a new sample, the nonlinear mapping is updated with the moving window approach, as shown in Fig. 4. Initially, with the arrival of new sample, the training set will be updated to $N + 1$ samples. Accordingly, the incremental algorithm calculate Ψ_{N+1}^{-1} for the updated training set of $N + 1$ samples by using Ψ_N^{-1} and (8), without the matrix inversion and decrement algorithm computes Ψ_N^{-1} for the new training set from Ψ_{N+1}^{-1}, as shown in (9). The size of nonlinear mapping (Ψ_N^{-1}) will thus remain fixed as N. As the main purpose of this algorithm is for real-time applicability, only new sample (data pair) is augmented to the existing training set as and when the new sample arrives in real-time. As the incremental algorithm augments the single data pair, the decremental algorithm discards the oldest single data pair. The parameters α and b for the updated N data pairs are obtained from (5) and the corresponding output can be predicted from (6). Flowchart representation of the procedure employed for multistep prediction of tremor with MWLS-SVM is shown in Fig. 4. With this procedure, the method does not require the prior knowledge of the delay as required in earlier methods.

TABLE I
OPTIMAL RANGES FOR C AND σ^2 SELECTION WITH VARIOUS VALUES OF N

N		C	σ^2	$\%Accuracy$
150	S	80 to 120	$< 10^{-1}$	$58 \pm 2\%$
	NS	80 to 120	$< 10^{-1}$	$59 \pm 2\%$
250	S	90 to 100	$< 10^{-2}$	$59 \pm 2\%$
	NS	90 to 100	$< 10^{-2}$	$68 \pm 2\%$
500	S	90 to 100	$< 10^{-2}$	$74 \pm 1\%$
	NS	90 to 100	$< 10^{-2}$	$76 \pm 1\%$
1000	S	80 to 100	$< 10^{-2}$	$75 \pm 1\%$
	NS	80 to 100	$< 10^{-2}$	$75 \pm 2\%$
2000	S	80 to 100	$< 10^{-2}$	$77 \pm 1\%$
	NS	80 to 100	$< 10^{-2}$	$78 \pm 2\%$

S - Surgeons and NS - Novice subjects

III. RESULTS

In this section, we first discuss the parameter selection procedure of MWLS-SVM for tremor prediction. Later, the performance analysis in comparison with existing methods are discussed.

In this paper, to quantify the performance we employ %accuracy, defined as

$$\%\text{accuracy} = \frac{\text{RMS}(s) - \text{RMS}(e)}{\text{RMS}(s)} \times 100$$

where root mean squares (RMS)$(s) = \sqrt{(\sum_{k=1}^{k=m}(s_k)^2/m)}$, m is the number of samples, s_k is the input signal at instant k, and e is the prediction error between actual signal and predicted signal.

A. Parameter Selection

Performance of MWLS-SVM relies on the appropriate initialization of the parameters: regularization constant (C), RBF kernel variance (σ), the number of training samples (N), and the signal history for regression (n). For initialization, a study was conducted on tremor data of all subjects and trials over a range of values for all parameters.

1) Selection of C and σ^2: C affects the prediction accuracy. Small magnitude of C yields an inaccurate regression model to fit the training data, whereas a large magnitude of C results in over-fitting. The mapping of data from low dimensional to high dimensional space is then performed with the kernel functions. Thus tuning the parameter σ^2 in RBF kernel is vital. To identify the optimal initialization for the hyper parameters, we initially performed a grid search (analysis on variations in prediction accuracy for multistep prediction as described in Section II-C) separately for both surgeons and novice subjects with exponentially increasing values for (C, σ^2) i.e., $10^0 < C < 10^4$ and $10^{-9} < \sigma^2 < 10^0$. Based on the results obtained with the wider range of values for the hyper parameters, a region of values with better prediction accuracy was then identified and an exhaustive grid search was conducted on the selected region. Based on the better prediction accuracy values, the finer grid region identified for tremor prediction was $20 < C < 200$ and $10^{-6} < \sigma^2 < 10^0$. For further information, refer to the supplementary materials of this paper.

Authorized licensed use limited to: Huazhong University of Science and Technology. Downloaded on September 23,2024 at 07:33:24 UTC from IEEE Xplore. Restrictions apply.

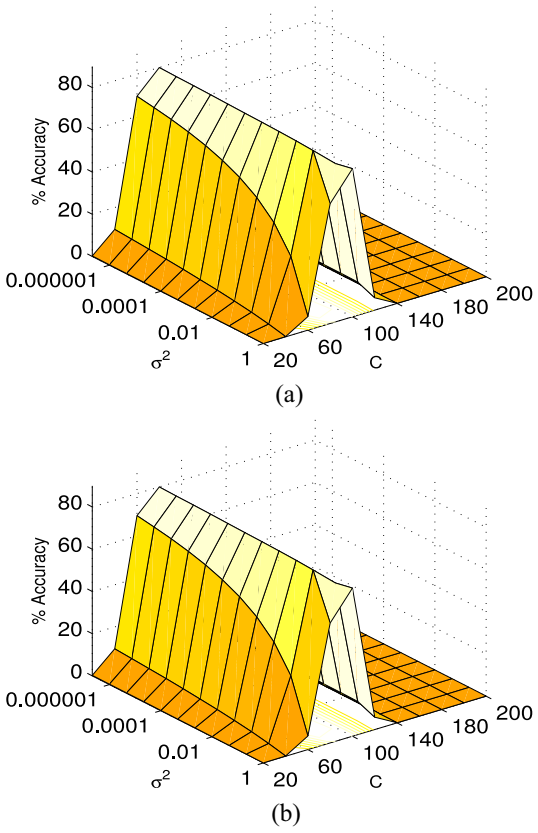

Fig. 5. Grid analysis of %accuracy for various values of C and σ^2; N = 500. (a) Surgeon's group. (b) Novice subject's group.

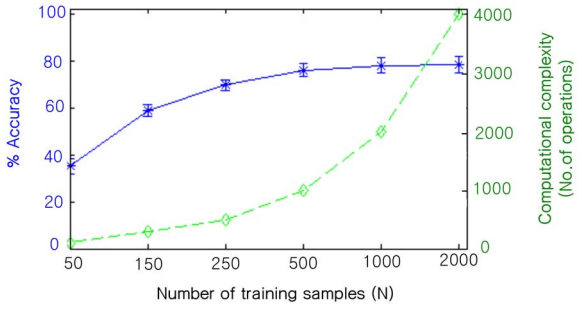

Fig. 6. Selection of signal history for offline training. Computational complexity (number of operations) of MWLS-SVM for every iteration (green in color).

Results obtained with the finer grid for hyper parameters and various values for N are tabulated in Table I. Results show that the region $80 \leq C \leq 100$ and $\sigma^2 \leq 0.01$ ensure stability and accuracy for both the groups. For illustration, the analysis conducted with N = 500 is shown in Fig. 5. The plots represent the average accuracy obtained for all subjects and trials in the corresponding group.

2) Selection of Signal History (Window Length): In MWLS-SVM, the window length selected for training determines the efficacy of algorithm. Training with less number of samples provides inaccurate prediction whereas a large set increases the computational complexity. To identify the optimal number of training samples (N), a study was conducted for multistep prediction with various values for N. The computational complexity for MWLS-SVM (number of operations for every iteration) is in the order of $\mathcal{O}(2N)$. The results obtained are shown in Fig. 6. Results show that $N = 500$ is the optimal number that yields good %accuracy and requires less computational complexity. The input vector length is selected based on the autocorrelation factor [27] and is identified as $n = 12$ for selected $N = 500$.

To evaluate the performance, the proposed approach is compared with the existing methods BMFLC-KF, AR-KF, and LS-SVM. Methods employed together with their parameters are tabulated in Table II.

TABLE II
METHODS AND PARAMETERS

Method	Parameters & initial conditions
WFLC-KF [21]	$f_0 = 7$ Hz; $\mu_1 = 5.10^{-4}$; $M = 1$; $R = 0.01$; $\mathbf{Q} = 0.01 \times \mathbf{I}$; $\mathbf{P}_0 = 0.01 \times \mathbf{I}$;
BMFLC-KF [8]	$\omega_1 - \omega_n = 7 - 14$ Hz; $\Delta\omega = 0.1$; $R = 0.01$; $\mathbf{Q} = 0.01 \times \mathbf{I}$; $\mathbf{P}_0 = 0.01 \times \mathbf{I}$;
AR-KF [5]	$M = 3$; $\mathbf{w}_0 = [-2.88, 2.83, -0.94]$; $R = 0.001$; $\mathbf{Q} = 0.01 \times \mathbf{I}$; $\mathbf{P}_0 = 0.001 \times \mathbf{I}$;
MWLS-SVM and LS-SVM	$N = 500$; $C = 100$; $\sigma = 0.0001$; $n = 12$;

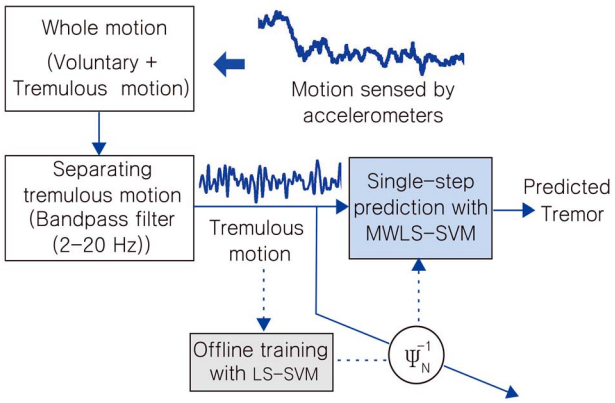

Fig. 7. Single-step prediction with MWLS-SVM.

B. Simulation Results

In this section, the performance of MWLS-SVM is evaluated with collected tremor data thru simulations followed by experimental results in the next subsection.

To highlight the robustness and suitability of MWLS-SVM for tremor prediction, as compared to the standard LS-SVM, an analysis is presented for single-step prediction in the first part of this section. In [5], it was shown that BMFLC-KF and AR-KF outperformed other methods for single-step prediction. To validate the proposed method, comparative performance is included. In the later part of this section, multistep prediction with MWLS-SVM for both known delay and unknown delay (frequency dependent) are analyzed. The comparison with the existing multistep prediction methods [8] is also presented.

1) Single-Step Prediction: The procedure employed to perform single-step prediction with MWLS-SVM is shown in Fig. 7. Fifth order Butterworth bandpass filter with a pass band

Authorized licensed use limited to: Huazhong University of Science and Technology. Downloaded on September 23,2024 at 07:33:24 UTC from IEEE Xplore. Restrictions apply.

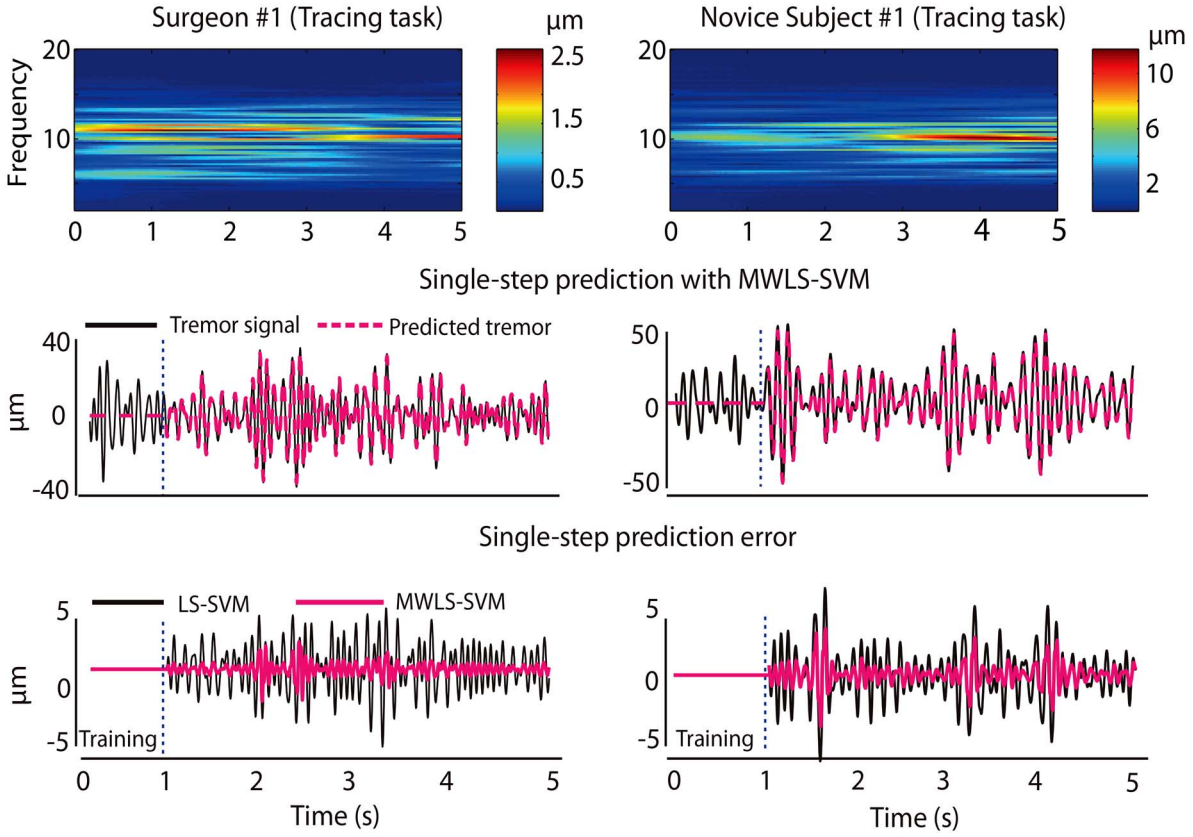

Fig. 8. Performance of MWLS-SVM and LS-SVM for single-step prediction.

of 2–20 Hz is employed to separate the tremulous motion from the whole motion as shown in Fig. 7. Single-step prediction is then performed on the filtered tremor data. To perform single-step prediction with MWLS-SVM, first N samples of data is considered for offline training. With the training set, the mapping Ψ_N^{-1} and the parameters α and b are computed offline with (5). LS-SVM performs single-step prediction with the fixed α and b computed in offline, whereas MWLS-SVM performs prediction by updating the parameters α and b at every iteration as described in Fig. 4. %accuracy (mean $\pm$ standard deviation) obtained with MWLS-SVM and LS-SVM for both the groups (surgeons and novice subjects) over all trials is tabulated in Table III. Results show that MWLS-SVM provides improved performance compared to LS-SVM.

For illustration, the results obtained with LS-SVM and MWLS-SVM for surgeon #1 (tracing task) and novice subject #1 (tracing task) are shown in Fig. 8. It is evident from Fig. 8, MWLS-SVM has relatively less error compared to the standard LS-SVM. Furthermore, Fig. 8 (spectrogram) highlights the robustness of MWLS-SVM to the variations in the tremor frequency band and bandwidth.

Comparative analysis with existing methods for both the groups are also tabulated in Table III. The parameters chosen for all the existing methods are provided in Table II. Results show that MWLS-SVM also provides a good prediction accuracy. It can be seen from Table III, BMFLC-KF and AR-KF provide the best prediction accuracy.

2) Multistep Prediction With Known Delay: To analyze the performance of MWLS-SVM for multistep prediction of tremor, we introduced a known delay corresponding to various prediction lengths [4 ms (two samples), 8 ms, 16 ms, and 20 ms (ten samples)] into the procedure as shown in Fig. 9. A bandpass filter is employed to separate tremulous motion from the whole motion. For instance, to perform two samples ahead prediction, a delay of 4 ms will be introduced thru the induced delay stage as shown in Fig. 9.

TABLE III
COMPARISON ANALYSIS WITH EXISTING SINGLE-STEP PREDICTION METHODS

Method	Surgeons	Novice subjects
WFLC-KF [21]	92.43 ± 0.64	91.43 ± 0.52
BMFLC-KF [15]	99.97 ± 0.002	99.98 ± 0.002
AR-KF [5]	99.61 ± 0.11	99.23 ± 0.12
LS-SVM	94.51 ± 2.56	92.47 ± 1.52
MWLS-SVM	96.47 ± 1.52	97.47 ± 0.82

For MWLS-SVM, initial N samples of tremor signal and the corresponding T samples ahead values are provided for offline training. With the training set, the parameters α and b are calculated from (5). The multistep prediction will be performed with (6) from the $N+1$ sample onward. The procedure to update the parameters α and b for every iteration with MWLS-SVM is described in Fig. 4.

Results of the proposed method MWLS-SVM were compared with the existing methods MS-BMFLC-KF, MS-AR-KF [8] and conventional LS-SVM. Task-wise analysis was conducted on both surgeons and novice subjects data. Results are shown in Figs. 10 and 11. In Fig. 10(a)–(d), task-wise prediction accuracy (with standard deviation) for

Authorized licensed use limited to: Huazhong University of Science and Technology. Downloaded on September 23,2024 at 07:33:24 UTC from IEEE Xplore. Restrictions apply.

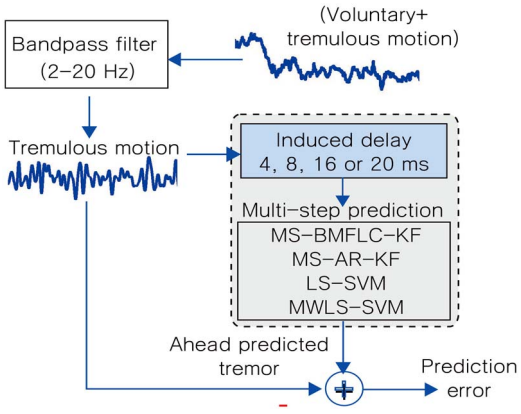

Fig. 9. Multistep prediction with various induced delays for all methods.

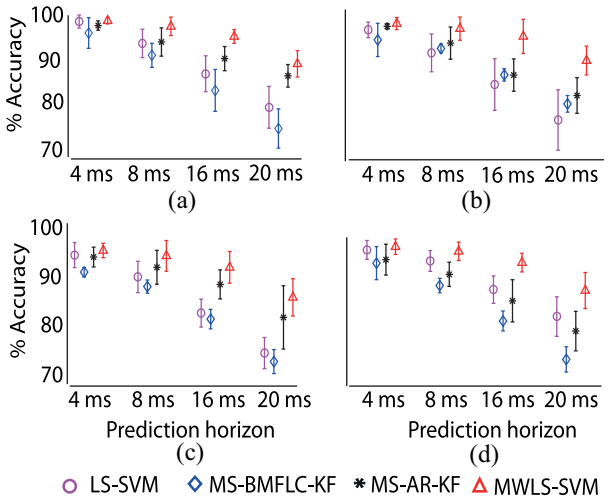

Fig. 10. Multistep prediction performance in the presence of various induced delays. Novice subjects: (a) tracing task and (b) pointing task. Surgeons: (c) tracing task and (d) pointing task.

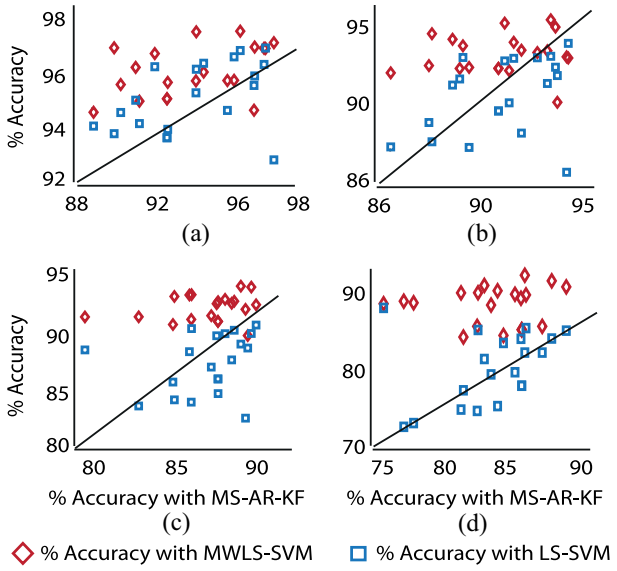

Fig. 11. Scatter plots. Prediction horizon: (a) 4 ms, (b) 8 ms, (c) 16 ms, and (d) 20 ms.

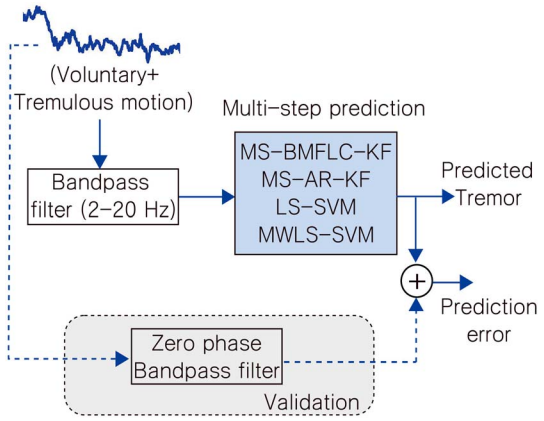

Fig. 12. Multistep prediction in the presence of unknown delay.

all delays and all methods is shown. It can be seen that MWLS-SVM performs better than all the other methods.

To further highlight the robustness in prediction performance with MWLS-SVM compared to MS-AR-KF and conventional LS-SVM, scatter plots for all delays obtained with the three methods are shown in Fig. 11(a)–(d). Each marker represents, the average prediction accuracy over all the six trials of a subject. For comparison, %accuracy obtained with MS-AR-KF is set as the reference (x-axis). For e.g., if a diamond marker lies above the diagonal line, it denotes that MWLS-SVM outperforms MS-AR-KF for that particular subject. Further, if a diamond marker of a subject is above the square marker of the corresponding subject, it denotes that MWLS-SVM provides better prediction accuracy than conventional LS-SVM. From the scatter plots, one can clearly see that as prediction horizon increases, the diamond markers (MWLS-SVM) separate from the square markers and distributed above the diagonal line. Hence, it can be inferred that MWLS-SVM performs better and is more robust for large prediction lengths compared to the rest.

3) Multistep Prediction With Unknown Delay (Frequency Dependent Delay): To analyze the performance of MWLS-SVM in the presence of unknown delay, a fifth-order Butterworth bandpass filter with pass band 2–20 Hz is employed for filtering tremulous component from voluntary motion as shown in Fig. 12. Based on the surgeon's frequency characteristics, this filter introduces a phase delay in the range of 12–16 ms into the procedure. As discussed earlier, MWLS-SVM based prediction relies on the nonlinear mapping and does not require the knowledge of the prediction length (horizon). Existing multistep prediction methods MS-BMFLC-KF and MS-AR-KF can only be formulated for a known prediction length. For analysis, the prediction length 20 ms is fixed for both MS-BMFLC-KF and MS-AR-KF methods similar to [8]. A zero phase band pass filter with same specifications as band pass filter was then employed to obtain the tremor signal without any phase delay and this serves as ground truth to compare the performance.

For illustration, the prediction errors obtained with all methods for surgeon #1 (pointing task) in the presence of unknown delay are shown in Fig. 13. The tremor signal and the prediction error obtained due to delay are shown in Fig. 13(a) and (b), respectively. The results obtained with multistep prediction methods (MS-BMLFC-KF, LS-SVM,

Authorized licensed use limited to: Huazhong University of Science and Technology. Downloaded on September 23,2024 at 07:33:24 UTC from IEEE Xplore. Restrictions apply.

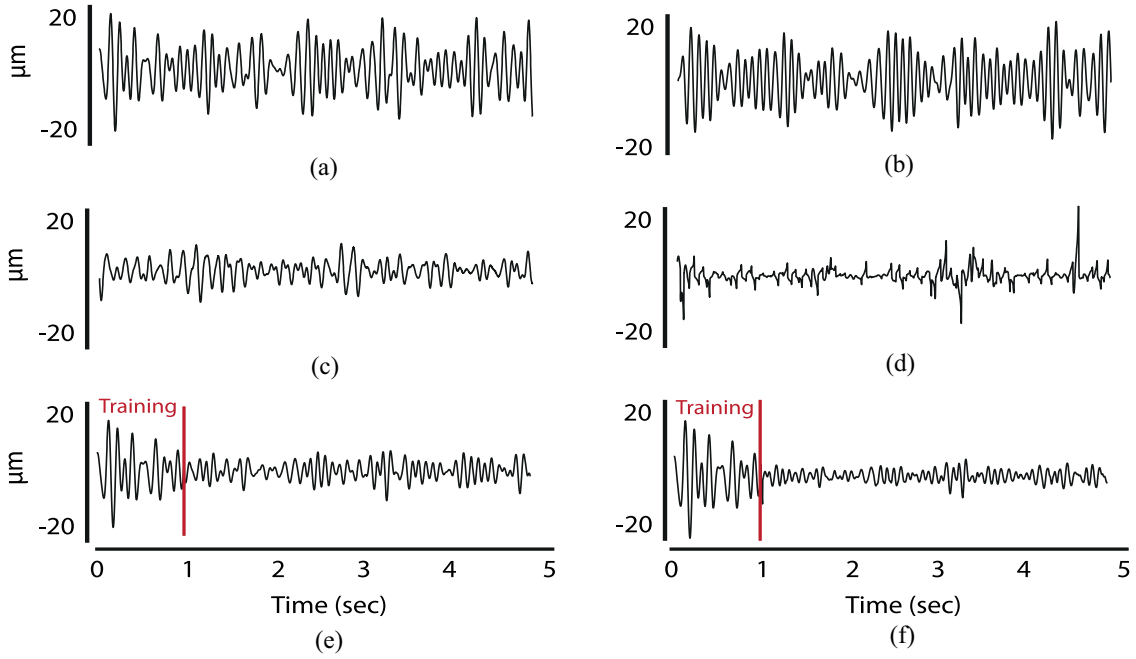

Fig. 13. (a) Surgeon #1 (pointing task). (b) Prediction error due to unknown delay. (c) Prediction error with MS-BMFLC-KF. (d) Prediction error with LS-SVM. (e) Prediction error with MS-AR-KF. (f) Prediction error with MWLS-SVM.

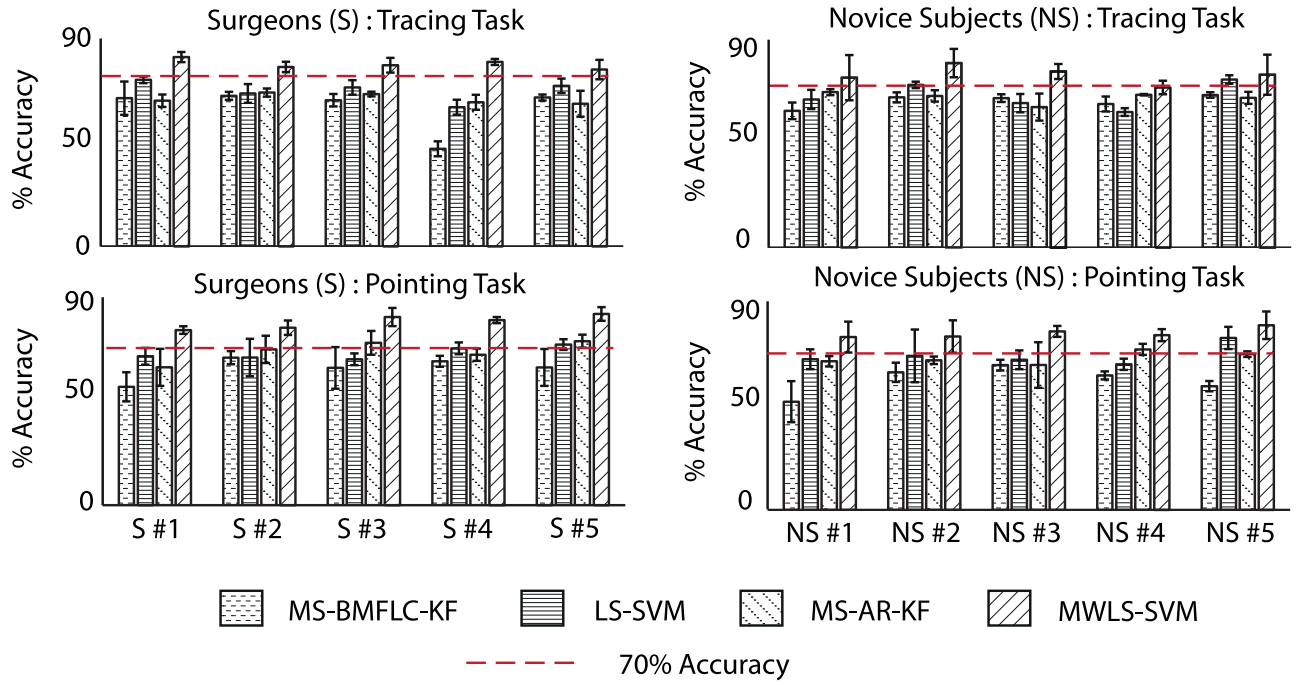

Fig. 14. Performance analysis of all methods in the presence of unknown delay.

MS-AR-KF, and MWLS-SVM) are shown in Fig. 13(c)–(f), respectively. The results show that MWLS-SVM has less prediction error compared to the other multistep prediction methods.

To quantify the performance, subject-wise analysis with all methods was conducted on the whole database. As subjects require more control, they displayed huge variations in tremor amplitude while performing tracing task compared to pointing task. Hence, the analysis was conducted separately for the two tasks. As pointing task is less complex compared to tracing task, %accuracy obtained for pointing task is higher than the %accuracy obtained with tracing task, as shown in Fig. 14. The subject-wise comparative analysis with all methods in the presence of frequency dependent delay is shown in Fig. 14. The dotted line in the plots indicates prediction accuracy of 70%. It can be clearly seen that MWLS-SVM provides better performance compared to existing methods for both the subject groups and tasks. For instance, MWLS-SVM provides

Authorized licensed use limited to: Huazhong University of Science and Technology. Downloaded on September 23,2024 at 07:33:24 UTC from IEEE Xplore. Restrictions apply.

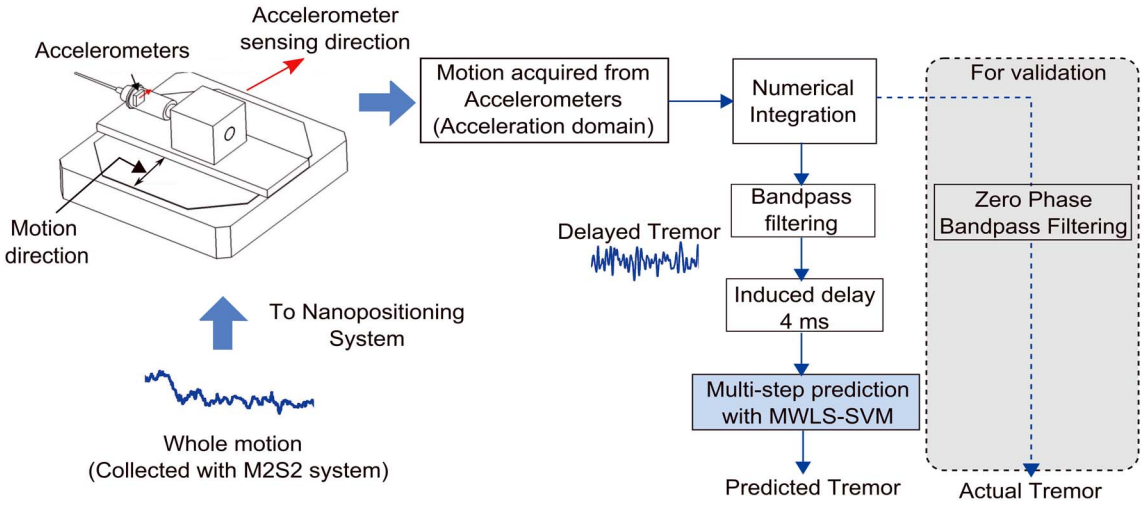

Fig. 15. Experimental procedure.

an average %accuracy of 75.96 ± 2.85% for surgeon's pointing task compared to 68.26 ± 1.58% with MS-AR-KF. On average of 7% improvement was obtained with the proposed method compared to the earlier methods.

C. Experimental Validation

The procedure employed for experimental validation is shown in Fig. 15. The tremor compensation instrument (Itrem [34]) which contains accelerometers (ADXL 203, analog devices, USA), was mounted on the nanopositioning stage (P-561.3CD from Physik Instrumente, Germany) as shown in Fig. 15. Further, the nanopositioning stage was driven in one axis to regenerate the tremor motion within 100 nm, the maximum range of the stage. A detailed study was performed in [19] to compare the real-tremor motion with the tremor obtained thru numerical double integration from the accelerometers. For more information about the experimental set up validation, refer to [15], [19], and [34]. The orientation of accelerometer along with the direction motion are shown in the schematic diagram (Fig. 15). For more information about the placement of accelerometers in the tremor compensation instrument, see [34]. The voltage output from the accelerometer was acquired at 500 Hz using a 16-bit data acquisition (DAQ) card (PD2-MF-150, United Electronic Industries, Inc., USA). With a quadratic function, the acquired voltage readings from accelerometer were converted to acceleration [34].

Experiments are conducted with data of three subjects [surgeon #1 (tracing task), surgeon #2 (pointing task), novice subject #1 (tracing task)] with two trials per subject. Parameters and initial conditions for real-time experiments are similar to the simulation experiments. In [8], MS-AR-KF provided better performance compared to existing methods for multistep prediction. Further based on our study in an earlier section (Section III-B, Fig. 14), we infer that MS-AR-KF provides better performance compared to standard LS-SVM. Hence for experimental validation, we only choose MS-AR-KF and MWLS-SVM. To evaluate the performance of both methods, the phase corrected tremulous motion obtained

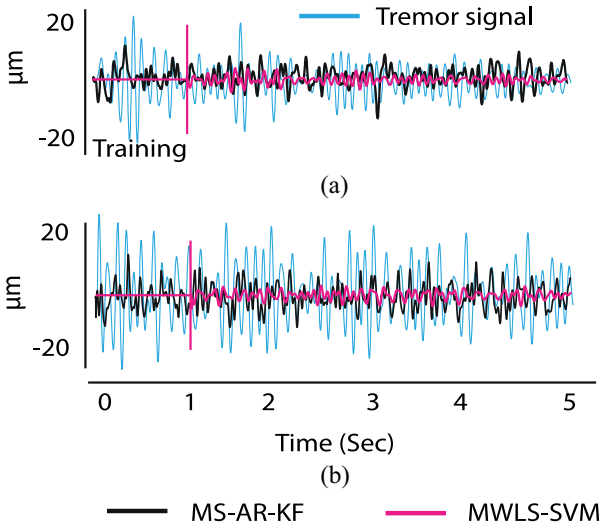

Fig. 16. Prediction performance in presence of unknown delay (a) tracing task of surgeon #1 and (b) tracing task of novice subject #1.

with zero phase band pass filter (in offline) was employed. For illustration, results obtained with tremor data of surgeon #1 (tracing task) and Novice subject #1 (tracing task) are shown in Fig. 16. For comparison, the multistep prediction error obtained with both methods MS-AR-KF and MWLS-SVM are shown together. From Fig. 16, it can be clearly seen that prediction error with MWLS-SVM is small compared to MS-AR-KF. Similar results for novice subject's tremor data are presented in Fig. 16(b). Overall for three subjects data, an average %accuracy of 71 ± 1.89% was obtained with MWLS-SVM, whereas 64 ± 2 was obtained with MS-AR-KF.

IV. Discussion

The tremor prediction methods are being developed as part of our continuing research in developing hand-held robotics devices for canceling tremor. The device consists of three accerelometers for sensing the tip acceleration of *x*-, *y*-, and *z*-axes separately [19]. Although 1-degrees of freedom (DOF) cancellation is discussed in this paper, the proposed method

Authorized licensed use limited to: Huazhong University of Science and Technology. Downloaded on September 23,2024 at 07:33:24 UTC from IEEE Xplore. Restrictions apply.

can be applied for the three axes separately and 3-DOF cancellation of tremor can be achieved. For sake of the performance analysis and testing, 1-DOF motion prediction is presented in this paper.

The major factor that affects the performance of hand-held instruments in real-time is the phase delay due to linear filters. Furthermore, microsurgery involves a lot of complex gestures, for e.g., an intentional sudden jerk caused by a surgeon is a huge challenge for identification and filtering in real time. Due to the presence of inertial sensors unwanted high-frequency noise and unwanted quadratic drift that results from conversion of acceleration to position are added to the signal. As the voluntary motion, noise and integration drift can be separated in the frequency domain, a band-pass filter can successfully filter the tremor motion from those unwanted components in the whole motion.

The standard LS-SVM requires a matrix inversion of order N to update the training set with the new sample at every iteration. The computational complexity (number of multiplications) to implement a matrix inversion is in the order of $\mathcal{O}(N^3)$. In MWLS-SVM, both the increment and decrement algorithms only rely on matrix multiplications and removes the requirement of matrix inversion. This reduces the computational complexity to the order of $\mathcal{O}(2N)$ for every iteration. Further, with the update of the nonlinear mapping online, MWLS-SVM can track the nonstationary dynamics of tremor signal more effectively. The issues related to nonstationary characteristics of tremor and computational complexity can be addressed with the proposed formulation.

Although existing methods MS-BMFLC-KF and MS-AR-KF provide good accuracy in real-time, the prediction horizon should be known *a priori*. The delay arising in the tremor compensation due to band-pass filtering depends on the instantaneous frequency of the tremor. As surgeon's display control over the tremor, the frequency band is distributed and hence the delay can be time-varying. The MWLS-SVM on the other hand relies on updating the nonlinear mapping at every iteration and the method adapts to the time-varying characteristics of tremor. The main advantage of the proposed approach lies in the fact that it does not require the knowledge of prediction horizon.

Existing literature on the robotics based compensation of tremor suggests that final compensation of 70% will be ideal for microsurgery to improve the surgeon's performance [4], [19], [36]. With the existing single-step prediction methods (BMFLC [4] and AR [5]), although the tremor prediction accuracy was high, the over all end compensation accuracy of the instrument in bench tests was significantly lower (around 40 to 50%) and depends on several other factors [4], [5]. Analysis showed that the loss in end compensation accuracy was more due to phase delay, integration drift and other sensor noises. In this paper, we have addressed the phase delay problem and the prediction performance is improved by nearly 10% compared to the existing multistep prediction methods [8]. With this improvement, we foresee that the final compensation accuracy during instrument trials will be improved. The final tests that are planned in future with micro surgeons will reveal the actual performance of the instrument.

The proposed method can be successfully applicable to many other applications such as classification of tremor profiles, prediction of pathological tremor, prediction of respiratory motion etc besides physiological tremor compensation. These problems will be discussed elsewhere.

V. Conclusion

As a solution to overcome the unknown phase delay in hand-held instruments, multistep prediction with kernel-based learning technique (MWLS-SVM) is developed in this paper. The analysis conducted on the tremor data demonstrated that the proposed method MWLS-SVM performs better compared to the existing methods for known and unknown prediction horizons. To evaluate the suitability of MWLS-SVM for real-time applications, the approach is evaluated experimentally in comparison with existing methods. Results show that an average %accuracy of $71 \pm 1.89\%$ is obtained with the proposed approach in comparison to $64 \pm 2\%$ obtained with the existing MS-AR-KF method.

References

[1] R. J. Elbe and W. C. Koller, *Tremor*. Baltimore, MD, USA: John Hopkins Univ. Press, 1985.

[2] R. Taylor *et al.*, "A steady-hand robotic system for microsurgical augmentation," *Int. J. Robot. Res.*, vol. 18, no. 12, pp. 1201–1210, 1999.

[3] S. Charles, *Computer Integrated Surgery: Technology and Clinical Applications*. Cambridge, MA, USA: MIT Press, 1996, ch. Dexterity Enhancement for Surgery.

[4] K. C. Veluvolu and W. T. Ang, "Estimation and filtering of physiological tremor for real-time compensation in surgical robotics applications," *Int. J. Med. Robot. Comput. Assist. Surg.*, vol. 6, no. 3, pp. 334–342, 2010.

[5] S. Tatinati, K. C. Veluvolu, S. M. Hong, W. T. Latt, and W. T. Ang, "Physiological tremor estimation with autoregressive (AR) model and Kalman filter for robotic applications," *IEEE Sensors J.*, vol. 13, no. 12, pp. 4977–4985, Dec. 2013.

[6] L. M. S. Eileen *et al.*, "Micromanipulation accuracy in pointing and tracing investigated with a contact-free measurement system," in *Proc. 31st IEEE Annu. Int. Conf. Eng. Med. Biol. Soc. (EMBS)*, Minneapolis, MN, USA, 2009, pp. 3960–3963.

[7] W. T. Latt, K. C. Veluvolu, and W. T. Ang, "Drift-free position estimation of periodic or quasi-periodic motion using inertial sensors," *Sensors*, vol. 11, no. 6, pp. 5931–5951, 2011.

[8] K. C. Veluvolu, S. Tatinati, S. M. Hong, and W. T. Ang, "Multistep prediction of phyisological tremor for surgical robotic applications," *IEEE Trans. Biomed. Eng.*, vol. 60, no. 11, pp. 3074–3082, Nov. 2013.

[9] S. Kozelj and S. N. Baker, "Different phase delays of peripheral input to primate motor cortex and spinal cord promote cancellation at physiological tremor frequencies," *J. Neurophysiol.*, vol. 111, pp. 2001–2016, Feb. 2014.

[10] G. Grimaldi, A. Frenandez, and M. Manto, "Augmented visual feedback counteracts the effect of surface muscular functional electrical stimulation on physiological tremor," *J. Neuroeng. Rehabil.*, vol. 10, pp. 1–12, Sep. 2013.

[11] T. Heida, E. C. Wentink, and E. Marani, "Power spectral density analysis of physiological, rest and action tremor in Parkinson's disease patients treated with deep brain stimualtion," *J. Neuroeng. Rehabil.*, vol. 10, pp. 1–11, Jun. 2013.

[12] S. Morrison, N. Cortes, K. M. Newell, and G. Kerr, "The pattern of coupling dynamics between postual motion, isotonic hand movements and physiological tremor," *Neurosci. Lett.*, vol. 580, pp. 41–46, Sep. 2014.

[13] G. Deuschl, J. Raethjen, and M. Lindemann, "The pathophysiology of tremor," *Muscle Nerve*, vol. 24, no. 6, pp. 716–735, 2001.

[14] C. N. Riviere, W. T. Ang, and P. K. Khosla, "Toward active tremor canceling in handheld microsurgical instruments," *IEEE Trans. Robot. Autom.*, vol. 19, no. 5, pp. 793–800, Oct. 2003.

[15] K. C. Veluvolu and W. T. Ang, "Estimation of physiological tremor from accelerometers for real-time applications," *Sensors*, vol. 11, no. 3, pp. 3020–3036, 2011.

Authorized licensed use limited to: Huazhong University of Science and Technology. Downloaded on September 23,2024 at 07:33:24 UTC from IEEE Xplore. Restrictions apply.

[16] B. Carignan, J. F. Daneault, and C. Duval, "The organization of upper limb physiological tremor," *Eur. J. Appl. Physiol.*, vol. 112, no. 4, pp. 1269–1284, 2012.
[17] A. P. L. Bo, P. Poignet, and C. Geny, "Pathological tremor and voluntary motion modeling and online estimation for active compensation," *IEEE Trans. Neural Syst. Rehabil. Eng.*, vol. 19, no. 2, pp. 177–185, Apr. 2011.
[18] W. T. Ang, C. N. Riviere, and P. K. Khosla, "An active hand-held instrument for enhanced microsurgical accuracy," in *Medical Image Computing and Computer-Assisted Intervention—MICCAI 2000*, vol. 1935. Berlin, Germany: Springer, Oct. 2000, pp. 878–886.
[19] W. T. Latt, U. X. Tan, C. Y. Shee, C. N. Riviere, and W. T. Ang, "Compact sensing design of a handheld active tremor compenstaion instrument," *IEEE Sensors J.*, vol. 9, no. 12, pp. 1864–1871, Dec. 2009.
[20] K. A. Mann, F. W. Werner, and A. K. Palmer, "Frequency spectrum analysis of wrist motion for activites of daily living," *J. Orthop. Res.*, vol. 7, no. 2, pp. 304–306, 1989.
[21] J. A. Gallego, E. Rocon, J. O. Roa, J. C. Moreno, and J. L. Pons, "Real-time estimation of pathological tremor parameters from gyroscope data," *Sensors*, vol. 10, no. 3, pp. 2129–2149, 2010.
[22] C. M. Bishop, *Pattern Recognition and Machine Learning*, M. Jordan, J. Klienberg, and B. Scholkopf, Eds. New York, NY, USA: Springer, 2007.
[23] F. Lotte, M. Congedo, A. Lecuyer, F. Lamarche, and B. Arnaldi, "A review of classification algorithms for EEG-based brain-computer interfaces," *J. Neural Eng.*, vol. 4, no. 2, pp. R1–R13, 2007.
[24] Y. Tian, Z. Qi, X. Ju, Y. Shi, and X. Liu, "Nonparallel support vector machines for pattern classification," *IEEE Trans. Cybern.*, vol. 44, no. 7, pp. 1067–1079, Jul. 2014.
[25] W. Kim, J. Park, J. Yoo, H. J. Kim, and C. G. Park, "Target localization using ensemble support vector regression in wireless sensor networks," *IEEE Trans. Cybern.*, vol. 43, no. 4, pp. 1189–1198, Aug. 2013.
[26] Y. Pang, K. Zhang, Y. Yaun, and K. Wang, "Distributed object detection with linear SVMs," *IEEE Trans. Cybern.*, vol. 44, no. 11, pp. 2122–2133, Nov. 2014.
[27] F. Ernst and A. Schweikard, "Forecasting respiratory motion with accurate online support vector regression (SVRpred)," *Int. J. Comput. Assist. Radiol. Surg.*, vol. 4, no. 5, pp. 439–447, 2009.
[28] J. Ma, J. Thelier, and S. Perkins, "Accurate online support vector regression," *Neural Comput.*, vol. 15, no. 11, pp. 2683–2703, 2003.
[29] G. Cauwenberghs and T. Poggio, *Advances in Neural Information Processing System*, T. K. Leen, T. G. Dietterich, and V. Tresp, Eds. Cambridge, MA, USA: MIT press, 2001.
[30] N. I. Sapankevych and R. Shankar, "Time series prediction using support vector machines: A survey," *IEEE Comput. Intell. Mag.*, vol. 4, no. 2, pp. 24–38, May 2009.
[31] S. Tatinati, Y. Wang, G. Shafiq, and K. C. Veluvolu, "Online LS-SVM based multi-step prediction of physiological tremor for surgical robotics," in *Proc. 35th IEEE Annu. Int. Conf. Eng. Med. Biol. Soc. (EMBS)*, Osaka, Japan, 2013, pp. 6043–6046.
[32] J. A. K. Suykens, J. Vandewalle, and B. De Moor, "Optimal control by least squares support vector machines," *Neural Netw.*, vol. 14, no. 1, pp. 23–35, 2001.
[33] J. A. K. Suykens, T. Van Gestel, J. De Brabanter, B. De Moor, and J. Vandewalle, *Least Squares Support Vector Machines*. Singapore: World Scientific, 2002.
[34] W. T. Latt *et al.*, "A micro motion sensing system for micromanipulation tasks," *Sensors Actuat. A Phys.*, vol. 173, no. 1, pp. 254–266, 2012.
[35] G. H. Golub and C. F. Van Loan, *Matrix Computations*. Baltimore, MD, USA: Johns Hopkins Univ. Press, 1989.
[36] C. N. Riviere, J. Gangloff, and M. Mathelin, "Robotic compensation of biological motion to enhance surgical accuracy," *Proc. IEEE*, vol. 94, no. 4, pp. 1706–1716, Sep. 2006.

Sivanagaraja Tatinati (S'13) received the B.Tech. degree in electronics and communication engineering from Acharya Nagarjuna University, Guntur, India, in 2010. He is currently pursuing the Ph.D. degree from Kyungpook National University, Daegu, Korea.

His current research interests include robotics assisted medical instruments, adaptive filtering, machine learning techniques based regression, and application of estimation and prediction algorithms in bio-medical engineering.

Kalyana C. Veluvolu (S'03–M'06–SM'13) received the B.Tech. degree in electrical and electronic engineering from Acharya Nagarjuna University, Guntur, India, and the Ph.D. degree in electrical engineering from Nanyang Technological University, Singapore, in 2002 and 2006, respectively.

Since 2009, he has been with the College of IT Engineering, Kyungpook National University, Daegu, Korea, where he is currently an Associate Professor. From 2006 to 2009, he was a Research Fellow with Biorobotics Group, Robotics Research Center, Nanyang Technological University. His current research interests include nonlinear estimation and filtering, sliding mode control, brain-computer interface, biomedical signal processing, and surgical robotics.

Wei Tech Ang (S'98–M'04) received the B.E. and M.E. degrees in mechanical and production engineering from Nanyang Technological University, Singapore, in 1997 and 1999, respectively, and the Ph.D. degree in robotics from Carnegie Mellon University, Pittsburgh, PA, USA, in 2004.

Since 2004, he has been with the School of Mechanical and Aerospace Engineering, Nanyang Technological University, where he is currently an Associate Professor and the Head of the Engineering Mechanics Division. His current research interests include robotics technology for biomedical applications, which include surgery, rehabilitation, and cell micromanipulation.

Authorized licensed use limited to: Huazhong University of Science and Technology. Downloaded on September 23,2024 at 07:33:24 UTC from IEEE Xplore. Restrictions apply.